J Mater Sci (2009) 44:1187–1191
DOI 10.1007/s10853-009-3268-3

Hydrothermal synthesis and magnetic properties of $NiFe_2O_4$ nanoparticles and nanorods

Qi Liu · Hexiang Huang · Lifang Lai · Jianhua Sun · Tongming Shang · Quanfa Zhou · Zheng Xu

Received: 21 April 2008 / Accepted: 13 January 2009 / Published online: 4 February 2009

Abstract $NiFe_2O_4$ nanoparticles and nanorods were synthesized by a facile hydrothermal treatment of $Ni(DS)_2$ (Nickel dodecyl sulfate), $FeCl_3$, and NaOH aqueous solution at 120 °C. The products were characterized by powder X-ray diffraction, transmission electron microscopy, and selected area electron diffraction. The magnetic properties were evaluated using a vibrating sample magnetometer. The probable mechanism of the formation of $NiFe_2O_4$ nanoparticles and nanorods was discussed.

Introduction

Spinel ferrites (MFe_2O_4; M = Fe, Co, Ni, Mn, Zn) have recently attracted a great deal of attention, due to both the broad practical applications in several important fields such as electronic devices, information storage, magnetic resonance imaging (MRI), drug-delivery technology, catalysis [1–10], and fundamental understanding of unusual properties of nanoparticles compared to those of bulk materials. The intrinsic properties of a spinel ferrite nanoparticle are mainly determined by its composition, size, and shape [9, 10]; so, it is desirable to develop strategies for shape-controlled synthesis of magnetic spinel ferrites. Because of the practical reasons mentioned above, the synthesis of nanostructured $NiFe_2O_4$ has also attracted considerable attention. Various methods have been developed to synthesize nanocrystalline $NiFe_2O_4$, including a sonochemical process [11], precursor techniques [12, 13], coprecipitation [14], mechanical alloying [15], sol–gel [16–18], pulsed wire discharge [19], shock wave [20], reverse micelle [21], hydrothermal [22] and ultrasonically assisted hydrothermal processes [23], polymer-pyrolysis route [24], mechano-chemical synthesis (mechanosynthesis) [25, 26], ultrasonic nozzle spray in situ mixing and microwave-assisted preparation[27], egg white precursor route [28], combustion reaction [29]. However, there are only a few reports on the morphology-controlled synthesis of nickel ferrite nanomaterial. Chu et al. [30] prepared $NiFe_2O_4$ nanocubes and nanorods by a hydrothermal method. Zhang et al. [31] synthesized $NiFe_2O_4$ nanorods via a polyethylene glycol (PEG)-assisted route. Recently, we have synthesized nanometer and micrometer hollow nickel spheres, CuO nanoplatelets and nanorods, PbS cubic nanocrystals, and $CoFe_2O_4$ nanoplatelets via using metal dodecyl sulfate $M(DS)_2$ (M = Ni, Cu, Pb, Co) as both the reactant and the surfactant, respectively [32–36]. Herein, we report a novel method for the synthesis of $NiFe_2O_4$ nanoparticles and nanorods via hydrothermal treatment of aqueous solution of nickel dodecyl sulfate ($Ni(DS)_2$), $FeCl_3$, and NaOH at 120 °C.

Q. Liu (✉) · H. Huang · L. Lai
Department of Chemical Engineering and Key Laboratory of Fine Petro-chemical Technology, Jiangsu Polytechnic University, Changzhou, Jiangsu 213164, People's Republic of China
e-mail: liuqi62@163.com

J. Sun · T. Shang · Q. Zhou
Jiangsu Key Laboratory of Precious Metals Chemistry, Jiangsu Teachers University of Technology, Changzhou 213001, People's Republic of China

Z. Xu
State Key Laboratory of Coordination Chemistry and National Laboratory of Solid State Microstructure, Nanjing University, Nanjing, Jiangsu 210093, People's Republic of China

Experimental section

All the regents were of analytical purity, and were used without further purification. $Ni(DS)_2$ are made by mixing an aqueous of sodium dodecyl sulfate with nickel chloride, as described in the literature [37].

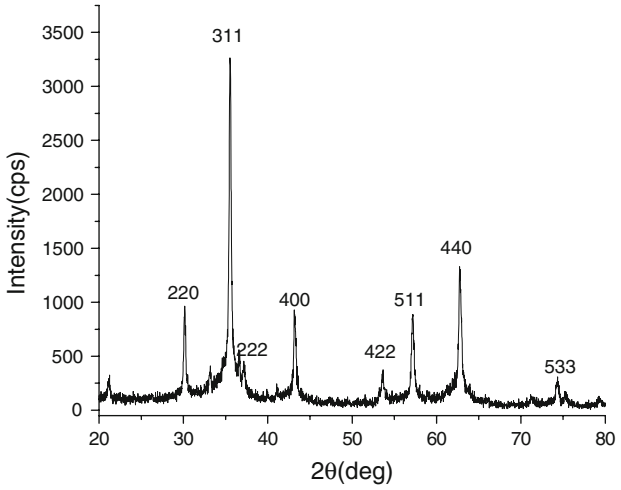

Fig. 1 XRD pattern of the $NiFe_2O_4$ nanocrystals obtained in the typical synthesis

The X-ray powder diffraction (XRD) pattern of the as-prepared products was collected on a Shimadzu XD-3A X-ray diffractometer with Cu Kα radiation ($\lambda = 0.15147$ nm). Transmission electron microscopy (TEM) images and selected area electron diffraction patterns (SAED) were obtained by employing JEOL JEM-200CX transmission electron microscope, using an accelerating voltage of 200 kV. Using a Lake Shore 7303-9309 vibrating sample magnetometer performed room-temperature magnetic characterization of the nanocrystals.

In a typical synthesis, $Ni(DS)_2$ (0.88 g) was added to 10 mL distilled water and stirred for a few minutes at 50 °C to ensure the complete dissolution of $Ni(DS)_2$ (the concentration of $Ni(DS)_2$ was 0.15 M), followed by the addition of $FeCl_3 \cdot 6H_2O$ (0.81 g) and stirred for the dissolution of $FeCl_3 \cdot 6H_2O$ (the concentration of $FeCl_3 \cdot 6H_2O$ was 0.30 M), then 10 mL aqueous solution of NaOH containing 1 g NaOH (the concentration of NaOH was 2.5 M) was added to the above solution and stirred for several minutes, and the resulting mixture was

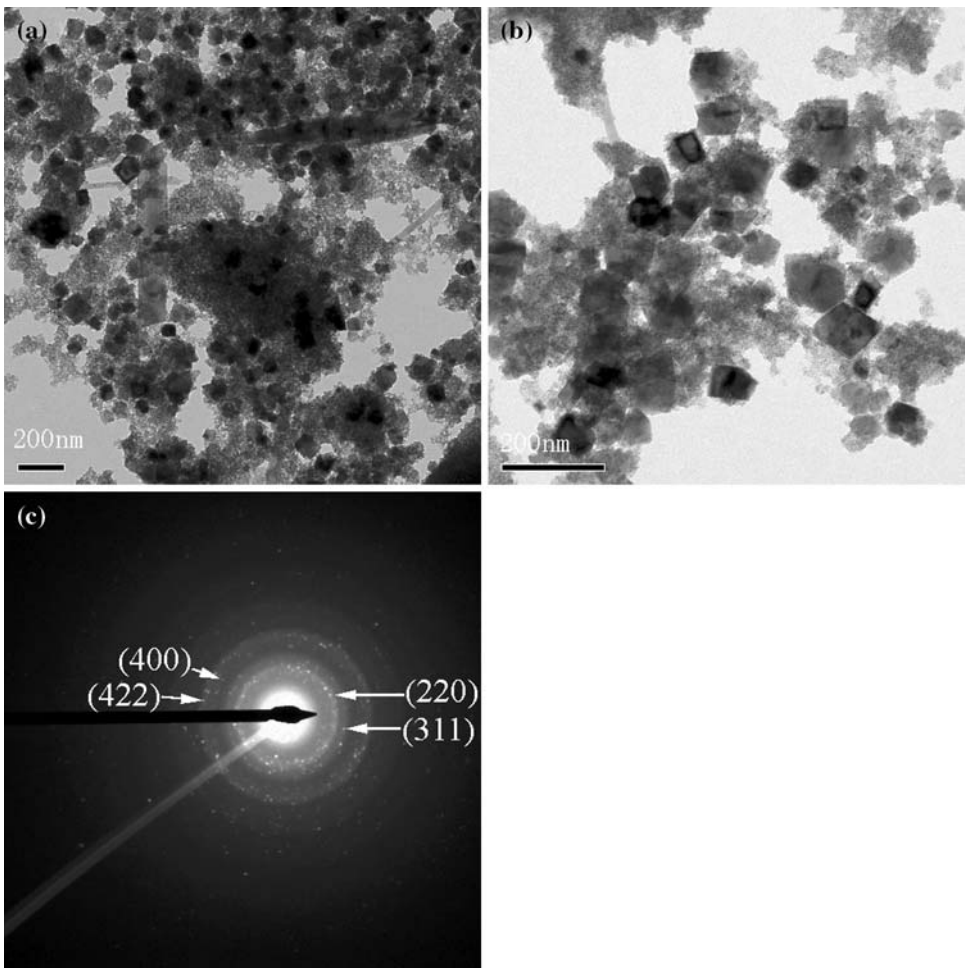

Fig. 2 **a** TEM image of the $NiFe_2O_4$ nanocrystals, **b** an enlarge image of the $NiFe_2O_4$ nanocrystals, and **c** SAED image of the $NiFe_2O_4$ nanocrystals obtained in the typical synthesis

poured into a 35 mL Teflon-lined stainless steel autoclave, sealed and maintained at 120 °C for 8 h. The black precipitates were collected, washed several times with distilled water, ethanol, and centrifuged. Finally, the products were dried in an oven at 60 °C temperature. $NiFe_2O_4$ nanocrystals (about 0.32 g) were obtained. The yield for the nanocrystals is above 90%.

Results and discussion

The XRD pattern of the prepared products is shown in Fig. 1. Eight characteristic peaks can be indexed as the cubic structure $NiFe_2O_4$, which is accorded with the reported data (JCPDS File No 10–0325). The peaks with 2θ values of 30.141, 35.559, 37.159, 43.179, 53.621, 57.199, 62.760, 74.320° correspond to the crystal planes (220), (311), (222), (400), (422), (511), (440), (533) of crystalline $NiFe_2O_4$, respectively.

The morphology and microstructure of the $NiFe_2O_4$ products were further examined with transmission electron microscopy (TEM), selected area electron diffraction (SAED). Figure 2a shows a typical TEM image of the $NiFe_2O_4$ products. The TEM image in Fig. 2a reveals that the products consist of many nanoparticles, some quasi nanocubes, and a few nanorods. Figure 2b is an enlarged image of the $NiFe_2O_4$ nanocrystals. The size of most $NiFe_2O_4$ nanoparticles is about in the range of 10–35 nm, while the size of some $NiFe_2O_4$ nanoparticles with morphology of quasi cube is about in the range of 45–115 nm. Figure 2c is a selected area electron diffraction pattern (SAED) acquired from the assembly of $NiFe_2O_4$ nanoparticles and quasi nanocubes. The diffraction rings being indexed correspond to the crystal plane (220), (311), (400), and (422) of $NiFe_2O_4$, respectively, showing that the products have crystalline spinel structure. Additional diffraction spots and rings of second phases have not been found in Fig. 2c, which may reveal that there is no oxide layer around the particles.

To learn more about the formation of $NiFe_2O_4$ nanoparticles and nanorods, we examined the effect of the hydrothermal reaction time and the concentration of $Ni(DS)_2$ and $FeCl_3 \cdot 6H_2O$ on the morphology and size of $NiFe_2O_4$ nanoparticles and nanorods. When the reaction

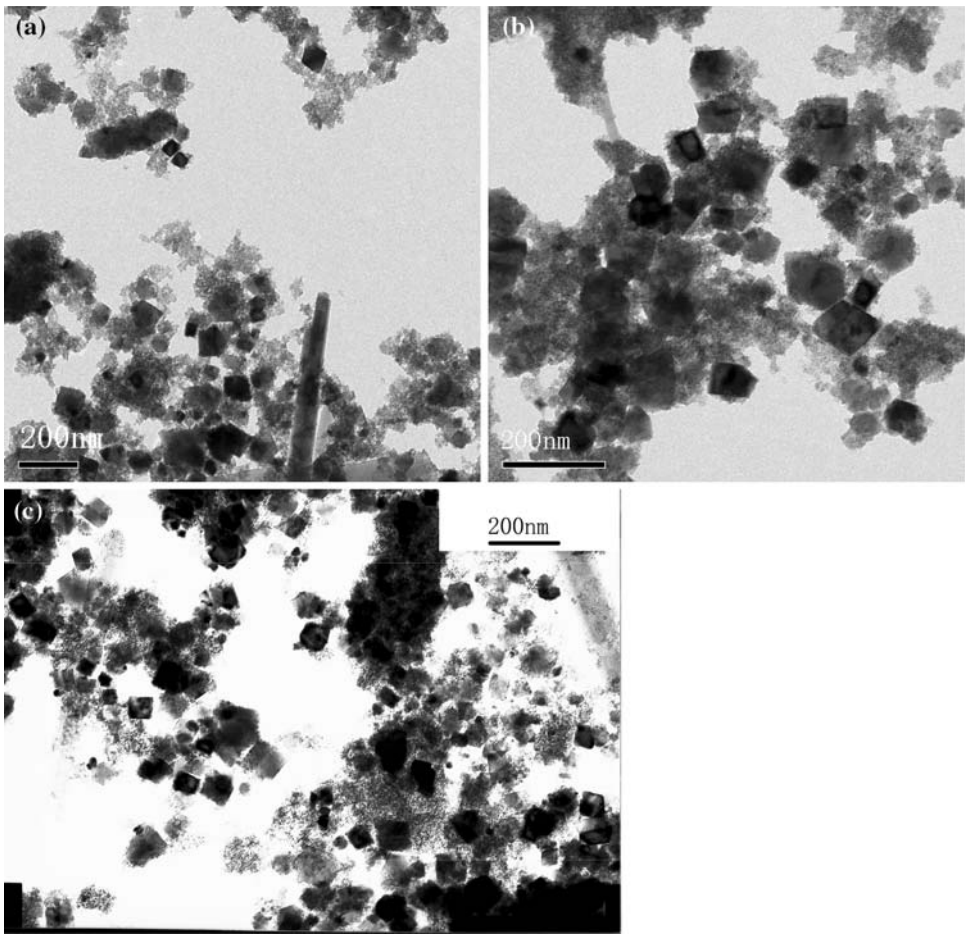

Fig. 3 TEM patterns of the $NiFe_2O_4$ nanocrystals obtained via hydrothermal treatment of $Ni(DS)_2$, $FeCl_3$, and NaOH solution at 120 °C for 4 h (**a**), 12 h (**b**), and 24 h (**c**). The concentration of $Ni(DS)_2$, $FeCl_3$, and NaOH was 0.15 M, 0.30 M, and 2.5 M, respectively

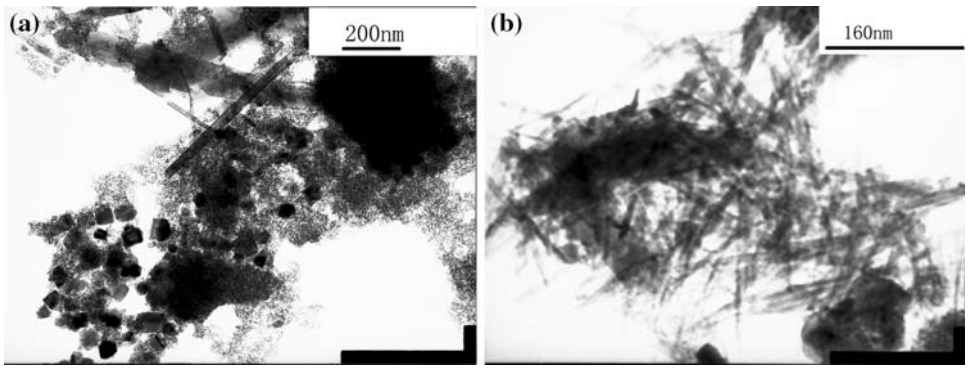

Fig. 4 TEM patterns of the $NiFe_2O_4$ nanocrystals obtained via hydrothermal treatment of $Ni(DS)_2$, $FeCl_3$, and NaOH solution at 120 °C for 8 h. The concentration of $Ni(DS)_2$, $FeCl_3$, and NaOH was 0.075 M, 0.15 M, and 2.5 M (**a**), and 0.26 M, 0.51 M, and 2.5 M, respectively (**b**)

time was 4, 12, and 24 h, respectively, and the other reaction conditions were kept unchanged, we found that all the products consisted of $NiFe_2O_4$ nanoparticles and a few nanorods (Fig. 3a, b, and c). When the concentration of $Ni(DS)_2$ and $FeCl_3 \cdot 6H_2O$ decreased to 0.075 and 0.15 M or increased to 0.26 and 0.51 M, respectively, and the other reaction conditions were kept unchanged, we found that all the products also consisted of $NiFe_2O_4$ nanoparticles and nanorods (Fig. 4a, b), and the size of the nanoparticles was also not obviously changed, but the amount of the nanorods increased with increasing concentration of $Ni(DS)_2$ and $FeCl_3 \cdot 6H_2O$ (Fig. 4b). Based on the facts, we speculate that the formation of $NiFe_2O_4$ nanoparticles and nanorods might be relevant to functionalized surfactant $Ni(DS)_2$ as a soft structural template. Usually, after the concentration of surfactant solution is higher than the critical micellar concentration (cmc), with the concentration of surfactant solution increasing, the spherical micelles are gradually changed into the rodlike micelles [34]. In our experimental system, the concentration of $Ni(DS)_2$ is higher than the critical micellar concentration (cmc) of $Ni(DS)_2$ (1.2×10^{-3} M) [37], which might favor some of the spherical micelles to change into rodlike micelles and result in the spherical and rodlike micelles coexisting in the system. Under hydrothermal condition, hydrophilic nickel ions from the spherical and rodlike micelles may react with Fe^{3+} and OH^- ions in the water, and form $NiFe_2O_4$ nanoparticles firstly, and then the nanoparticles are aggregated into the $NiFe_2O_4$ nanorods in the rodlike micelles. The detailed formation of the nanorods needs to be investigated further.

The magnetic properties of $NiFe_2O_4$ nanocrystals obtained in the typical synthesis were investigated with a vibrating sample magnetometer. Figure 5 shows the magnetization curves measured at 300 K for the $NiFe_2O_4$ nanocrystals obtained in the typical synthesis. The saturation magnetization (M_s), remanent magnetization (M_r), coercivity (H_c) are ca.30.4 emu g^{-1}, 4.8 emu g^{-1}, and 87.4 Oe for the $NiFe_2O_4$ nanocrystals at 300 K, respectively. The M_s of the $NiFe_2O_4$ nanocrystals is lower than

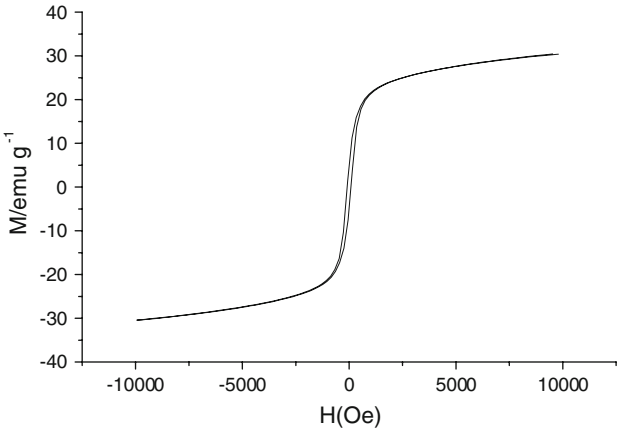

Fig. 5 Hysteresis loop of the $NiFe_2O_4$ nanocrystals obtained in the typical synthesis at 300 K

that of the corresponding bulk material (about 55 emu g^{-1}) [38]. Compared with the H_c value of bulk $NiFe_2O_4$ reported in literature (close to 0 Oe), the $NiFe_2O_4$ nanocrystals exhibit larger coercivity, which should be attributed to their nanostructure [39].

Conclusion

$NiFe_2O_4$ nanoparticles and nanorods have been successfully synthesized by a simple solution route using $Ni(DS)_2$ as both a precursor and a surfactant. Along with the increase of $Ni(DS)_2$ solution concentration, the amount of $NiFe_2O_4$ nanorods in the product also increased. The magnetic measurement shows that the $NiFe_2O_4$ nanocrystals obtained in the typical synthesis possess higher saturation magnetization (30.4 emu g^{-1}).

Acknowledgements We thank the National Natural Science Foundation of China (No. 20671045), the Natural Science Foundation of Education Department of Jiangsu Province (05KJB150023), the Natural Science Foundation of Jiangsu Key Laboratory of Precious Metals Chemistry of Jiangsu Teachers University of Technology, and the Natural Science Foundation of Jiangsu Province Key Laboratory of Fine Petro-chemical Technology of Jiangsu Polytechnic University for financial support.

References

1. Zhao W, Gu J, Zhang L, Chen H, Shi J (2005) J Am Chem Soc 127:8916
2. Caruso F, Spasova M, Susha A, Giersig M, Caruso RA (2001) Chem Mater 13:109
3. Hyeon T (2003) Chem Commun 927
4. Yu S, Yoshimura M (2002) Adv Funct Mater 12:9
5. Perez JM, Loughlin TO, Simeone FJ, Weissleder R, Josephson L (2002) J Am Chem Soc 124:2856
6. Perez JM, Simeone FJ, Tsourkas A, Josephson L, Weissleder R (2004) Nano Lett 4:119
7. Rashad MM, Fouad OA (2005) Mater Chem Phys 94:365
8. Ma LJ, Chen LS, Chen SY (2007) J Phys Chem Solids 68:1330
9. Sun S, Zeng H, Robinson DB, Ramoux S, Rice PM, Wang SX, Li G (2004) J Am Chem Soc 1246:273
10. Song Q, Zhang ZJ (2004) J Am Chem Soc 126:6164
11. Shafi KVPM, Koltypin Y, Gedanken A, Prozorov R, Balogh J, Lendvai J, Felner I (1997) J Phys Chem B 101:6409
12. Prasad S, Gajbhiye NS (1998) J Alloys Compd 265:87
13. Kurinec SK, Okeke N, Gupta SK, Zhang H, Xiao TD (2006) J Mater Sci 41:8181. doi:10.1007/s10853-006-0393-0
14. Yang JM, Tsuo WJ, Yen FS (1999) J Solid State Chem 145:50
15. Shi Y, Ding J, Liu X, Wang J (1999) J Magn Magn Mater 205:249
16. Chen D-H, He X-R (2001) Mater Res Bull 36:1369
17. Seyyed Ebrahimi SA, Azadmanjiri J (2007) J Non-Cryst Solids 353:802
18. Niu ZP, Wang Y, Li FS (2006) J Mater Sci 41:5726. doi:10.1007/s10853-006-0099-3
19. Kinemuchi Y, Ishizaka K, Suematsu H, Jiang W, Yatsui K (2002) Thin Solid Films 407:109
20. Liu J, He H, Jin X, Hao Z, Hu Z (2001) Mater Res Bull 36:2357
21. Kale A, Gubbala S, Misra RDK (2004) J Magn Magn Mater 277:350
22. Zhou J, Ma J, Sun C, Xie L, Zhao Z, Tian H (2005) J Am Ceram Soc 88:3535
23. Meskin PE, Ivanov VK, Barantchikov AE, Churagulov BR, Tretyakov YD (2006) Ultrason Sonochem 13:47
24. Liu X-M, Yang G, Fu S-Y (2007) Mater Sci Eng C 27:750
25. Yang H, Zhang X, Ao W, Qiu G (2004) Mater Res Bull 39:833
26. Šepelák V, Bergmann I, Feldhoff A, Heitjans P, Krumeich F, Menzel D, Litterst FJ, Campbell SJ, Becker KD (2007) J Phys Chem C 111:5026
27. Nyutu EK, Conner WC, Auerbach SM, Chen C-H, Suib SL (2008) J Phys Chem C 112:1407
28. Maensiri S, Masingboon C, Boonchomb B, Seraphin S (2007) Scr Mater 56:797
29. Costa CFM, Lula RT, Kiminami RHGA, Gama LFV, de Jesus AA, Andrade HMC (2006) J Mater Sci 41:4871. doi:10.1007/s10853-006-0048-1
30. Chu X-F, Jiang D-L, Zheng C-M (2007) Sens Actuators B 123:793
31. Zhang DE, Zhang XJ, Ni XM, Zheng HG, Yang DD (2005) J Magn Magn Mater 292:79
32. Liu Q, Liu H, Han M, Zhu J, Liang Y, Xu Z, Song Y (2005) Adv Mater 17:1995
33. Liu Q, Liu H, Liang Y, Xu Z, Yin G (2006) Mater Res Bull 41:697
34. Liu Q, Liang Y, Liu H, Hong J, Xu Z (2006) Mater Chem Phys 98:519
35. Liu Q, Ni Y, Yin G, Hong J, Xu Z (2005) Mater Chem Phys 89:379
36. Liu Q, Sun JH, Rong HR, Sun XQ, Zhong XJ, Xu Z (2008) Mater Chem Phys 108:269
37. Moroi Y, Motomura K, Matuura R (1974) J Colloid Interface Sci 46:111
38. Jiang J, Yang Y-M (2007) Mater Lett 61:4276
39. Liu J-H, Zhang L-F, Tian G-F, Li J-C, Li F-S (2007) Acta Phys Sin 56:6050